# Diffusion coefficient in periodic and random potentials

M. Khoury,[1] James P. Gleeson,[2] J. M. Sancho,[1] A. M. Lacasta,[3] and Katja Lindenberg[4]
[1]*Departament d'Estructura i Constituents de la Matèria, Facultat de Física, Universitat de Barcelona, Diagonal 647, E-08028 Barcelona, Spain*
[2]*Department of Mathematics and Statistics, University of Limerick, Limerick, Ireland*
[3]*Departament de Física Aplicada, Universitat Politècnica de Catalunya, Avinguda Doctor Marañon 44, E-08028 Barcelona, Spain*
[4]*Department of Chemistry and Biochemistry, University of California–San Diego, La Jolla, California 92093-0340, USA*
(Received 7 June 2009; published 26 August 2009)

Transport and diffusion of particles on modulated surfaces is a nonequilibrium problem which is receiving a great deal of attention due to its technological applications, but analytical calculations are scarce. In earlier work, we developed a perturbative approach to begin to provide an analytic platform for predictions about particle trajectories over such surfaces. In some temperature and forcing regimes, we successfully reproduced results for average particle velocities obtained from numerical simulations. In this paper, we extend the perturbation theory to the calculation of higher moments, in particular the diffusion tensor and the skewness. Numerical simulations are used to check the domain of validity of the perturbative approach.

DOI: 10.1103/PhysRevE.80.021123 PACS number(s): 05.60.Cd, 66.30.−h, 82.70.Dd, 05.40.−a

## I. INTRODUCTION

The response of particles in a thermal environment driven by external forces across modulated potential surfaces continues to pose interesting questions in theory, experiment, and simulations even though in many ways it may be considered a well-seasoned problem [1–18]. The motion of classical and of quantum particles over such surfaces exhibits a rich variety of behaviors that serves as a probe of surface structure and of the interplay of surface potentials, thermal motions, and directed forces that can be electrical, magnetic, or even of hydrodynamic origin. The most recent experimental interest arises because of the technological capabilities to use this response in the sorting or mixing of colloidal particles. Sorting of particles driven across modulated surfaces is a nondestructive technology that has successfully been implemented for separation of colloidal mixtures by size or by other particle characteristics. Not surprisingly, analytic results on this problem are limited. Our own previous work provides some of these results specifically in the context of particle sorting. In [18] we introduced a systematic perturbation procedure for characterizing the motion of particles over modulated surfaces when the external force driving the particle motion is large and/or the temperature of the medium is high. In these limits we were able to calculate the average velocity of the particles in both periodic and random potentials. In the context of particle sorting, we were particularly interested in extracting the direction of the average velocity relative to the direction of the external force and its dependence on particle parameters such as size. The agreement with numerical simulation results showed that our procedure has predictive value in the appropriate force and temperature regimes.

As we pointed out in our earlier work, the average velocity is but one feature of the distribution of particle positions and velocities, and our perturbation theory can be applied to the calculation of other interesting moments. One particular such moment is the diffusion tensor

$$D_{ij} = \frac{1}{2}\lim_{t\to\infty}\frac{d}{dt}\langle (x_i - \langle x_i\rangle)(x_j - \langle x_j\rangle)\rangle. \tag{1}$$

Here $x_i$ is the $i$ component of the displacement of particles from their initial positions and the brackets denote an ensemble average over thermal fluctuations. The diffusion tensor is thus a second moment of the particle displacements. In this paper we pursue the calculation of this tensor as well as that of the third moment (skewness) of the particle displacements based on our perturbative high-force high-temperature approach.

As in [18], we consider the motion of identical noninteracting particles moving on a surface described by a two-dimensional potential $V(x,y)$ which may be periodic or random. We implement the ubiquitous overdamped limit, so that the equations of motion for the components of the particle displacement are given by

$$\dot{x} = -\frac{\partial}{\partial x}V(x,y) + F\cos\theta + \sqrt{2\mathcal{T}}\xi_x(t),$$

$$\dot{y} = -\frac{\partial}{\partial y}V(x,y) + F\sin\theta + \sqrt{2\mathcal{T}}\xi_y(t). \tag{2}$$

In these Langevin equations, the dots denote time derivatives, $\mathcal{T}$ is the dimensionless temperature, and the thermal fluctuation terms $\xi_i(t)$ are Gaussian and $\delta$ correlated

$$\langle \xi_i(t)\xi_j(t')\rangle = \delta_{ij}\delta(t-t'). \tag{3}$$

The constant external force vector is

$$\mathbf{F} = F\cos\theta\mathbf{i} + F\sin\theta\mathbf{j}. \tag{4}$$

We will also consider the corresponding one-dimensional (1D) case where particles move on a line described by a potential $V(x)$ and the particle displacement is described by the single coordinate $x$.

It is useful to provide a brief summary of our previous work based on this model as well as a generalization of it that includes inertial forces (underdamped regime). In [13],

 

which was purely numerical, we analyzed the magnitude as well as direction of the average velocity vector as a function of particle size (as captured in the parameters of the potential), temperature, and magnitude and direction of the external force in the overdamped case. Our simple model reproduced the rich behavior noted in colloidal experiments that had been interpreted via considerably more complicated models. In [14–17] we studied numerically the transport and diffusion properties in different lattice geometries in both asymmetric and symmetric periodic surface potentials. We also studied the effects of friction. In this latter analysis we included situations where the friction is sufficiently low to highlight the role of inertial effects. Finally, in [18] we presented our first attempts at developing an analytic approach to the overdamped problem. In particular, we developed an approximation method to obtain analytic formulas for the average velocity of particles and demonstrated the validity of the approximation at high temperatures $\mathcal{T}$ and/or strong forcing $F$. We found good agreement with numerical simulations in the appropriate regimes and extended the regime of agreement through an adjustment to the simple perturbation expansion. In that work we considered random as well as periodic potentials and found particularly interesting general conditions that dictate whether or not a modulated surface lends itself to particle sorting.

In the work presented here we build on those previous results, with the goal of finding analytic results for the second and third moments of the distribution of particle displacements using the perturbative approximation scheme first introduced in [18]. The second moments are introduced via the diffusion tensor $D_{ij}$ defined in Eq. (1). The so-called parallel and perpendicular diffusion coefficients (as in [15], for example) are calculated from the tensor by introducing a unit vector $\mathbf{u}$ and forming the scalar

$$\mathbf{u}\cdot\mathbf{D}\cdot\mathbf{u}=\sum_{i,j=1}^{2}u_iD_{ij}u_j. \tag{5}$$

When $\mathbf{u}$ is parallel to the external force $\mathbf{F}$, this scalar is the parallel diffusion coefficient $D_{\|}$; when $\mathbf{u}$ is perpendicular to $\mathbf{F}$, we obtain the perpendicular diffusion coefficient $D_{\perp}$. We note that many interesting properties of the diffusion coefficients were obtained numerically in [14,15]. The numerical simulations of [14,15] include a finite friction coefficient, unlike the overdamped case considered here; however, we expect some applicability of overdamped results when the friction coefficient is large. One of our motivations for this work is the large disparity between the values of $D_{\|}$ and $D_{\perp}$ at temperature $\mathcal{T}=0.2$ as shown in Fig. 3 of [15]. We show here that the difference between the parallel and perpendicular diffusion coefficients depends on a number of factors, including the angle $\theta$ of the external force and the symmetry of the periodic potential, as well as $\mathcal{T}$ and $F$.

In Sec. II we give the (first-order) approximation for the diffusion tensor. Using an exact result for the one-dimensional periodic diffusion coefficient, we examine the validity of our approximation at various temperatures and forcing strengths. In the explored cases, we compare our analytical results to numerical simulations. Concentrating on the role of force and temperature, we proceed to find $D_{\|}$ and $D_{\perp}$ for periodic two-dimensional potentials as used in [15]. We also study the diffusion coefficient for one-dimensional random potentials. In Sec. III we demonstrate the capability of the approximation scheme to examine higher-order moments of the distribution of particle displacements [19]. In particular, we give a formula for the third moment and derive the skewness for particles moving in a one-dimensional periodic potential. Comments and conclusions are indicated in Sec. IV and technical details are in the Appendix.

## II. DIFFUSION COEFFICIENTS

The diffusion tensor $D_{ij}$ is calculated using the first-order approximation developed in [18] as

$$D_{ij}=\mathcal{T}\delta_{ij}+\frac{\mathcal{T}}{(2\pi)^{2d}}\int d\mathbf{k}k^2\hat{Q}(\mathbf{k})k_ik_j\frac{3(\mathbf{k}\cdot\mathbf{F})^2-\mathcal{T}^2k^4}{[(\mathbf{k}\cdot\mathbf{F})^2+\mathcal{T}^2k^4]^2}, \tag{6}$$

where $d$ stands for dimension. As in Sec. III of [18], this first-order approximation can be applied to motion in either periodic potentials or random potentials by an appropriate choice of the kernel $\hat{Q}(\mathbf{k})$. For periodic potentials, $\hat{Q}(\mathbf{k})$ is defined in terms of the Fourier transform $\hat{V}$ of the potential $V(\mathbf{x})$ as

$$\hat{Q}(\mathbf{k})=\hat{V}(\mathbf{k})\hat{V}(-\mathbf{k}). \tag{7}$$

For random potentials (and after disorder-averaging), the appropriate kernel in formula (6) is

$$\hat{Q}(\mathbf{k})=(2\pi)^d\hat{E}(\mathbf{k}). \tag{8}$$

Here $\hat{E}(\mathbf{k})$ is the energy spectrum of the potential, defined as the Fourier transform of the (disorder-averaged) correlation function of the potential (see Sec. IIIB of [18]). The derivation of formula (6) is nontrivial. It is detailed in the Appendix for the random case and is easily carried out in similar fashion for the periodic case.

### A. One-dimensional periodic potential

In one dimension, the tensor $D_{ij}$ given in Eq. (6) reduces to the scalar diffusion coefficient

$$D=\mathcal{T}\left\{1+\frac{1}{(2\pi)^2}\int dkk^2\hat{Q}(k)\frac{3F^2-\mathcal{T}^2k^2}{[F^2+\mathcal{T}^2k^2]^2}\right\}. \tag{9}$$

Here we concentrate on the periodic case with potential $V(x)=\cos(2\pi x)$, so the equation of motion is

$$\frac{dx}{dt}=F+2\pi\sin(2\pi x)+\sqrt{2\mathcal{T}}\xi(t) \tag{10}$$

(note the change of notation with respect to Ref. [18] where $U$ instead of $F$ was used). In the absence of the potential, the diffusion coefficient would simply be $D=\mathcal{T}$, so that it is convenient to highlight the deviations from this behavior by writing the diffusion coefficient from Eq. (9) for this potential in terms of the ratio $D/\mathcal{T}$,

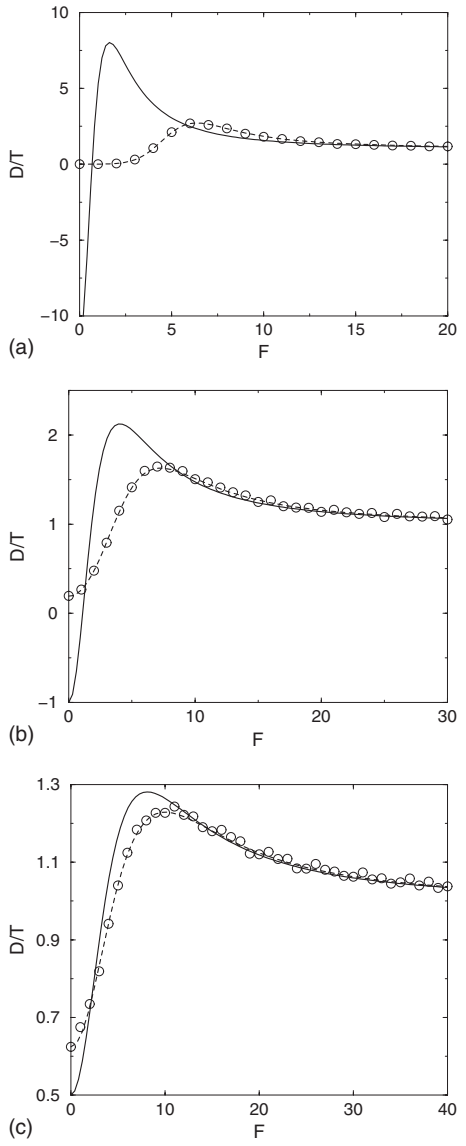


FIG. 1. Approximate (solid), exact (dotted), and numerical (symbols) 1D diffusion results for $D/\mathcal{T}$ as function of external force $F$ at temperatures (a) $\mathcal{T}=0.2$, (b) $\mathcal{T}=0.5$, and (c) $\mathcal{T}=1.0$.

$$\frac{D(F)}{\mathcal{T}} = 1 + 2\pi^2 \frac{3F^2 - 4\pi^2\mathcal{T}^2}{[F^2 + 4\pi^2\mathcal{T}^2]^2}. \tag{11}$$

In this particular instance, it is not necessary to use this approximate result for the diffusion coefficient because an exact result is available [20]. Nevertheless, we exhibit the comparison of this first-order approximation to the exact result given by Eq. (22) of [20] and to numerical simulation results to set a baseline for further comparisons. In Fig. 1, we compare the exact values of $D/\mathcal{T}$ (dotted line) versus the forcing $F$ to the first-order approximation (solid line) given by Eq. (11) at the three temperatures $\mathcal{T}=0.2$, 0.5, and 1.0. Consistent with our results for the mean velocity in [18], where we showed that the first-order approximation was useful for high temperatures and strong forcing, we find the same regimes of agreement here. Accordingly, we note in (a) and (b) of Fig. 1 the unphysically negative values of the approximate diffusion at low $F$ values when the temperature is low. At temperature $\mathcal{T}=1.0$, the agreement between the approximation and the exact result is good for all values of the forcing: this motivates our concentration on the case $\mathcal{T}=1.0$ in most of the examples to follow. Note also that in all cases, the approximate formula gives good predictions when the forcing $F$ is sufficiently large.

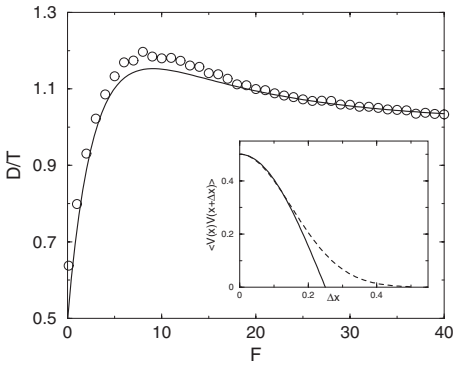


FIG. 2. Diffusion coefficient $D/\mathcal{T}$ as a function of force $F$ for a random one-dimensional potential with Gaussian energy spectrum. Parameters: $\varepsilon=0.188$, $\gamma=0.15$, and temperature $\mathcal{T}=1.0$. Analytic prediction (line) and numerical simulations (points). Inset: Potential correlation for a periodic case (solid line) and a Gaussian random one (dashed line).

### B. One-dimensional random potential

In the case of a random potential with Gaussian spatial correlations, the energy spectrum reads

$$\hat{E}(k) = \varepsilon e^{-k^2\gamma^2/2}, \tag{12}$$

as in Sec. V of [18]. Here $\gamma$ is the correlation length. The resulting diffusion constant is

$$\frac{D}{\mathcal{T}} = 1 + \frac{\varepsilon}{2\pi\mathcal{T}^5\gamma}\left[-\sqrt{2\pi}\mathcal{T}(\mathcal{T}^2 + 2F^2\gamma^2) + e^{F^2\gamma^2/2\mathcal{T}^2}\pi F\gamma(3\mathcal{T}^2 + 2F^2\gamma^2)\mathrm{erfc}\left(\frac{F\gamma}{\sqrt{2}\mathcal{T}}\right)\right], \tag{13}$$

which is plotted in Fig. 2 for $\mathcal{T}=1$ and compared to the numerical results obtained by simulating the equation of motion for a random potential with spectrum (12). The results are qualitatively very similar to those for the periodic case in Fig. 1 since the correlation functions are comparable in the two cases (as shown in the inset of Fig. 2) and are in good agreement with the numerical ones.

### C. Two-dimensional periodic potential

We consider motion on a two-dimensional surface with periodic potential given by the Fourier series

$$V(\mathbf{x}) = \sum_{n=0}^{M}\sum_{m=0}^{M} a_{nm}\cos(2\pi n x)\cos\left(2\pi m\frac{y}{\lambda}\right). \tag{14}$$

Note that this is a slight generalization of the potential used in [18] because the parameter $\lambda$ allows the periods in the $x$

and $y$ directions to be different. We use $\lambda=\sqrt{2}$ below to compare to the diffusion on the body-centered-cubic surface studied numerically in [15]. The effect of such a periodic potential on the diffusion in the direction of the unit vector $\mathbf{u}$ is given from the approximation (6) as

$$\frac{\mathbf{u}\cdot\mathbf{D}\cdot\mathbf{u}}{\mathcal{T}} = 1 + \frac{\pi^2}{2}\sum_{n=0}^{M}\sum_{m=0}^{M} a_{nm}^2 d_n d_m (n^2+\tilde{m}^2)[(nu_x+\tilde{m}u_y)^2 A_+ + (nu_x-\tilde{m}u_y)^2 A_-]. \tag{15}$$

We have used the abbreviations

$$A_\pm = \frac{3F^2(n\cos\theta \pm \tilde{m}\sin\theta)^2 - 4\pi^2\mathcal{T}^2(n^2+\tilde{m}^2)^2}{[4\pi^2\mathcal{T}^2(n^2+\tilde{m}^2)^2 + F^2(n\cos\theta\pm\tilde{m}\sin\theta)^2]^2} \tag{16}$$

and, for convenience, we have written $\tilde{m}$ in the sum term to stand for $m/\lambda$. For the parallel diffusion coefficient $D_\parallel$, the unit vector $\mathbf{u}$ has components $u_x=\cos\theta$, $u_y=\sin\theta$; for the perpendicular diffusion coefficient $D_\perp$, the components are $u_x=-\sin\theta$ and $u_y=\cos\theta$. The factors $d_n$ are defined as in [18]

$$d_n = 1+\delta_{0n} = \begin{cases} 2 & \text{if } n=0 \\ 1 & \text{if } n>0. \end{cases} \tag{17}$$

As an example for implementation, we take the potential with $a_{11}=1$ and all other $a_{nm}$ set to zero

$$V(x,y) = \cos(2\pi x)\cos\left(2\pi\frac{y}{\lambda}\right), \tag{18}$$

with $\lambda=\sqrt{2}$ [15]. We concentrate first on the high-temperature case $\mathcal{T}=1.0$, motivated by the good performance of the one-dimensional approximation at this temperature. Figure 3 shows $D_\parallel/\mathcal{T}$ (solid line) and $D_\perp/\mathcal{T}$ (dashed line) as a function of the forcing magnitude $F$. Recall that the direction of the forcing vector is determined by the angle $\theta$ [cf. Eq. (4)] and so we examine the effect of the angle $\theta$ by taking $\theta=0$ in Fig. 3(a), $\theta=\tan^{-1}\sqrt{2}$ (along the diagonal of the potential) in Fig. 3(b), and $\theta=\pi/2$ in Fig. 3(c). We note that in [15] the forcing vector is directed along the diagonal of the potential and that is the case of Fig. 3(b), where we remark two significant observations: the parallel diffusion exceeds the perpendicular and it shows a maximum around $F=10$.

The first observation depends on both the angle $\theta$ and the magnitude $F$ of the forcing vector: note from Fig. 3(c) that when the forcing is directed in the $y$ direction, $D_\perp$ exceeds $D_\parallel$ when $F$ is greater than approximately 8. In order to illustrate this effect in more detail, Fig. 4 shows the dependence of the parallel and perpendicular diffusion coefficients on the angle $\theta$ of the forcing vector at temperature $\mathcal{T}=1.0$ and fixed forcing magnitude $F=10$.

The figure demonstrates that $D_\perp$ is maximum along the $x$ and $y$ axes and minimum along the diagonal, while $D_\parallel$ does not exhibit significant variations as a function of forcing angle. Figure 4 also illustrates that this dependence is symmetric around $\theta=\pi/2$.

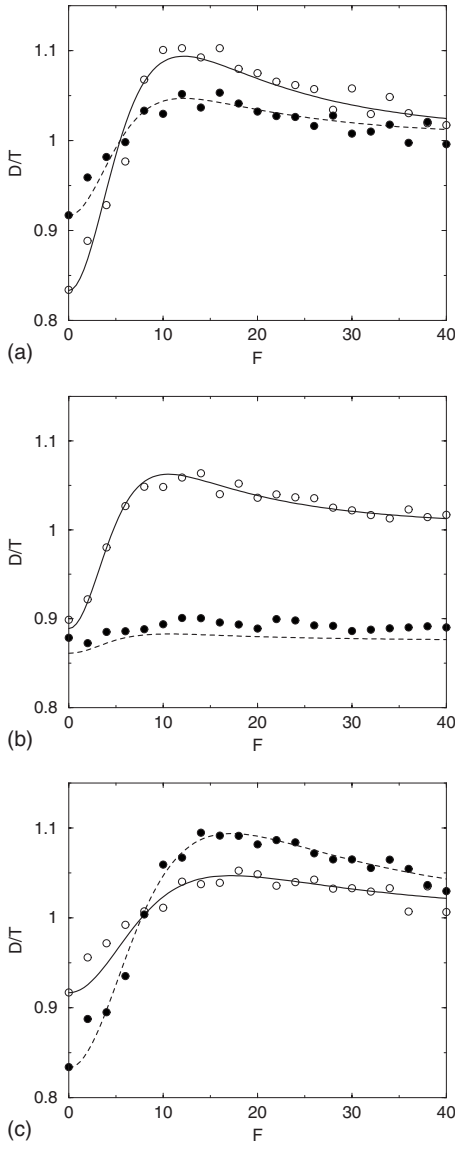


FIG. 3. Diffusion coefficients $D_\parallel/\mathcal{T}$ (solid and open) and $D_\perp/\mathcal{T}$ (dashed and filled) as functions of $F$, at temperature $\mathcal{T}=1.0$, and with the forcing vector at angles (a) $\theta=0$, (b) $\theta=\tan^{-1}\sqrt{2}$, and (c) $\theta=\pi/2$. Lines are results using our analytical approximation and points are numerical simulation results.

The second observation in Fig. 3(b), namely, the maximum in $D_\parallel$, can be understood if one realizes that diffusion is in some sense a measure of the variation of the average velocity with force magnitude $F$. In fact, for free Brownian motion there is an exact relation between the two, which in one dimension reads [21]

$$D = k_B T\frac{d\langle v\rangle}{dF}. \tag{19}$$

The value of $F$ for which $D_\parallel$ is a maximum in the presence of a periodic potential corresponds to the threshold between the *locked regime*, where forces are so low that particles hardly move, and the *transport regime*, where the magnitude of the force is sufficiently high for particles to essentially ignore the

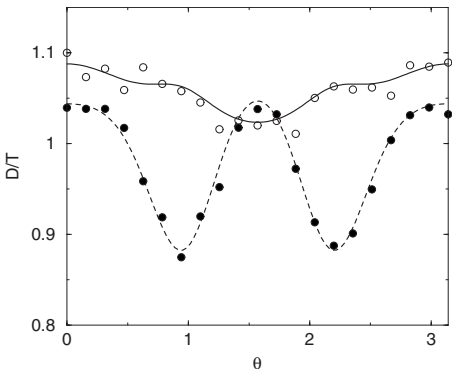


FIG. 4. Diffusion coefficients $D_{\|}/\mathcal{T}$ (solid and open) and $D_{\perp}/\mathcal{T}$ (dashed and filled) as functions of angle $\theta$ at temperature $\mathcal{T}=1.0$ and forcing magnitude $F=10$. Lines are approximate analytic results and points are numerical simulation results.

potential and simply follow the drift, thus acquiring the asymptotic average velocity $\langle v\rangle=F$.

We noted above that Fig. 3(b) bears a qualitative resemblance to Fig. 3 of [15] in that the parallel diffusion is larger than the perpendicular diffusion when the forcing vector is directed along the diagonal. The chief difference between Fig. 3(b) and the simulations in [15] (aside from the finite friction coefficient in the latter) is that the temperature in those simulations was $\mathcal{T}=0.2$, whereas here we use the higher temperature $\mathcal{T}=1.0$ to give improved validity to our approximation. Figure 5 shows the approximation results at the lower temperature $\mathcal{T}=0.2$. The forcing angle lies along the diagonal, $\theta=\tan^{-1}\sqrt{2}$. Note that $D_{\|}$ exhibits a range of unphysical negative values for low $F$ values, while $D_{\perp}$ is negative even at high values of $F$. This latter result is rather surprising, as we would naively have expected the quality of the approximation to improve as $F$ increases. To explain this, we carefully examine the formula (15) for the potential (18) in the case where the forcing vector points along the diagonal of the potential, i.e., $\theta=\tan^{-1}\lambda$. It can be shown that in this case, $D_{\|}$ may be written as

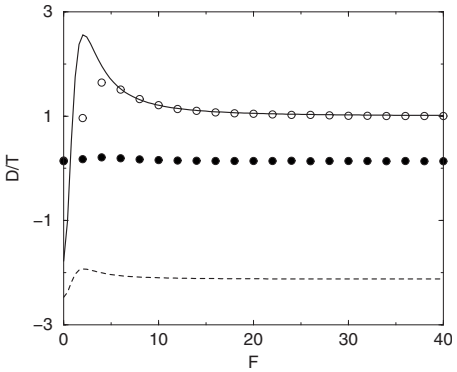


FIG. 5. Diffusion coefficients $D_{\|}/\mathcal{T}$ (solid and open) and $D_{\perp}/\mathcal{T}$ (dashed and filled) as functions of forcing magnitude $F$ at temperature $\mathcal{T}=0.2$ and angle $\theta=\tan^{-1}\sqrt{2}$. Lines are analytic results and points are numerical results.

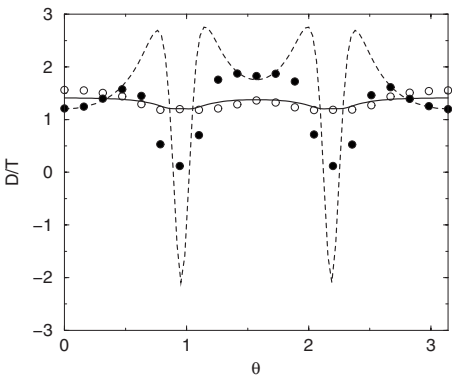


FIG. 6. Diffusion coefficients $D_{\|}/\mathcal{T}$ (solid and open) and $D_{\perp}/\mathcal{T}$ (dashed and filled) as functions of angle $\theta$ at temperature $\mathcal{T}=0.2$ and forcing magnitude $F=10$. Lines are approximate analytic results and points are numerical results.

$$\frac{D_{\|}}{\mathcal{T}} = 1 + \frac{\lambda^2}{(1+\lambda^2)^2} G\left(\frac{2\lambda^2 F}{(1+\lambda^2)^{3/2}}\right), \tag{20}$$

where the function $G(U)$ is defined in terms of the one-dimensional diffusion constant of Eq. (11) as

$$G(U) \equiv \frac{D(U)}{\mathcal{T}} - 1. \tag{21}$$

Similarly, the perpendicular diffusion coefficient may be related to the one-dimensional periodic case by

$$\frac{D_{\perp}}{\mathcal{T}} = 1 + \frac{1}{4}\frac{(1-\lambda^2)^2}{(1+\lambda^2)^2} G\left(\frac{2\lambda^2 F}{(1+\lambda^2)^{3/2}}\right) + \frac{1}{4}G(0). \tag{22}$$

The final term on the right-hand side of this equation involves evaluating the approximate one-dimensional diffusion constant when the forcing magnitude $F$ is zero. As Fig. 1(a) demonstrates, as $F$ approaches zero, the one-dimensional diffusion approximation has large negative values when the temperature is low. For instance, $G(0)=-12.5$ when $\mathcal{T}=0.2$. The effect of this $G(0)$ term on $D_{\perp}$ is therefore to cause the low-temperature values of the approximation to be in error even when the forcing magnitude $F$ is large. We therefore cannot make accurate analytic predictions for the perpendicular diffusion coefficient when the temperature is low, at least when the forcing direction is along the diagonal of the potential. Figure 6 shows the diffusion coefficients at temperature $\mathcal{T}=0.2$ and $F=10$ as functions of the angle $\theta$ of the forcing vector. The case studied above corresponds to $\theta=\tan^{-1}\sqrt{2}=0.955$, a direction in which $D_{\perp}$ is negative. As may be seen from the numerical results in Fig. 6, this unphysical prediction is an artifact of the theory (which may be ameliorated or removed at higher order).

## III. THIRD MOMENT AND SKEWNESS

The diffusion tensor is a measure of the second moment of the distribution of particle displacements. The techniques developed for the approximation of the second moment are generalizable to the study of the third and higher moments of the distribution, thus promising some insight into the non-

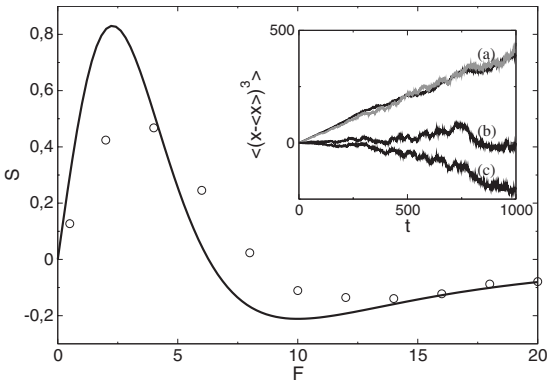


FIG. 7. The third moment coefficient $S$ as a function of $F$ for the one-dimensional periodic case at temperature $\mathcal{T}=1.0$. Inset: time evolution of the third moment of the displacement for different forces (a) $F=1$ (black) and $F=5$ (gray), (b) $F=8$, and (c) $F=10$.

Gaussian nature of the probability distribution. As a first step in this direction, we focus on the one-dimensional periodic potential of Sec. II A and calculate the first-order approximation to the third moment of the displacement distribution $\langle (x-\langle x\rangle)^3\rangle$. We find that after a sufficiently long time, this quantity grows linearly with time,

$$\langle (x-\langle x\rangle)^3\rangle \sim St \quad \text{as} \quad t\to\infty, \tag{23}$$

and the growth rate $S$ is given by

$$S=-96\pi^2 F\mathcal{T}^2\frac{F^2-4\pi^2\mathcal{T}^2}{[F^2+4\pi^2\mathcal{T}^2]^3}. \tag{24}$$

Figure 7 shows the coefficient $S$ as a function of forcing magnitude $F$ at temperature $\mathcal{T}=1.0$; note its negative values when $F$ is large. While exact results are known for the first two moments of the displacement distribution in the one-dimensional case [20], we are not aware of any exact (or even numerical) results for the third moment.

The fact that the third moment is nonzero means that the particle distribution is not Gaussian. A dimensionless measure of the deviation from Gaussianity is given by the skewness

$$\frac{\langle (x-\langle x\rangle)^3\rangle}{\langle (x-\langle x\rangle)^2\rangle^{3/2}} \sim \frac{S}{(2D)^{3/2}}t^{-1/2} \quad \text{as} \quad t\to\infty. \tag{25}$$

Our approximations thus predict that the skewness of the particle displacements distribution reverts to the Gaussian value of zero at sufficiently long times, but does so as $t^{-1/2}$. As follows from Eq. (24) and is illustrated in the inset of Fig. 7, the constant of proportionality $S$ is negative for large $F$ but becomes positive for smaller $F$. These predictions are tested via numerical simulations in Fig. 7.

## IV. COMMENTS AND CONCLUSIONS

In this paper we have continued our efforts to characterize the motion of particles over modulated surfaces driven by an external force or flow field. Our work is based on a systematic perturbation procedure introduced in [18], where we focused on calculating the direction of the average velocity relative to the direction of the external force and its dependence on particle parameters such as size. Here we have explored the diffusion tensor that measures the width of the distribution and the skewness that is a measure of the deviation of the distribution from a Gaussian. In particular, we have calculated the diffusion constant for one-dimensional random potentials as well as the two-dimensional diffusion coefficients $D_\parallel$ and $D_\perp$ for a periodic potential and have compared our results to those obtained from numerical simulations. We have also calculated the skewness for a one-dimensional periodic potential and show that it eventually vanishes for large $F$ values, thus indicating that the asymptotic distribution is Gaussian. However, the approach to zero is extremely stochastic, thus making numerical verification difficult.

In our earlier contribution we found that the theory worked well for the calculation of the average particle velocity when the external force driving the particle motion is large and/or the temperature of the medium is high. This is reasonable in view of the fact that the perturbation is carried out around the particle flow across a surface without a potential (flat surface). The opposite limit of low temperature and weak forcing corresponds to the Kramers "barrier-crossing" regime for which our theory is not appropriate. It is not surprising that here we again find that the first-order approximation to the higher moments works well at high temperatures and large forcing $F$, but worse results are found when both $F$ and $\mathcal{T}$ are low. The problems of the theory are more pronounced for the higher moments. In fact, we find unphysical results for $D_\perp$ at low temperatures even when $F$ is high and have traced this to an underlying relation between $D_\perp$ and the diffusion coefficient in a one-dimensional system at zero forcing.

A number of continuing directions for this work are envisioned. The application of the result in Eq. (6) to random two-dimensional potentials is straightforward and may provide interesting insights into the symmetry requirements for particle sorting. Not so straightforward algebraically but clearly desirable would be to develop higher-order approximations as was done in [18].

## ACKNOWLEDGMENTS

This work is supported in part by Science Foundation Ireland under Investigator Award No. 06/IN.1/I366 and MACSI (J.P.G.), by the MCyT (Spain) under Project No. FIS2006-11452 (J.M.S., A.M.L., and M.K.) and Grant No. FPU-AP2005-4765 (M.K.), and by the U.S. National Science Foundation under Grant No. PHY-0354937 (K.L.).

## APPENDIX

In this appendix we develop the approximate expression Eq. (6) for the diffusion tensor following the systematic approximation scheme introduced in [18]. The diffusion tensor as defined by Eq. (1) involves the calculation of some averages. We will do it by finding the coefficients in the long-time asymptotic forms

$$\langle x_i x_j \rangle \sim a_2^{ij} t^2 + a_1^{ij} t + o(t) \quad \text{as} \quad t \to \infty, \tag{A1}$$

$$\langle x_i \rangle \sim b_1^i t + b_0^i + o(1) \quad \text{as} \quad t \to \infty. \tag{A2}$$

We will show later that the combination $a_2^{ij} - b_1^i b_1^j$ that would lead to a quadratic time contribution of the moments (and hence to a ballistic contribution to the motion) is in fact zero, so that

$$D_{ij} = \frac{1}{2}[a_1^{ij} - b_0^i b_1^j - b_0^j b_1^i]. \tag{A3}$$

To calculate the coefficients in Eqs. (A1) and (A2), we will need the concentration of particles $c(\mathbf{x},t)$ that obeys the Fokker-Planck equation, Eq. (5) in Ref. [18]. In that work, an approximate solution to this equation was developed by considering Laplace and Fourier transforms of $c(\mathbf{x},t)$ in time and space, respectively. The first-order solution, expression (A10) in [18], can be written in $d$ dimensions as

$$\begin{aligned}\bar{c}(\mathbf{k},s) = P_s(\mathbf{k}) - \frac{i}{(2\pi)^d} P_s(\mathbf{k}) \int d\mathbf{p}\mathbf{k}\cdot\hat{\mathbf{u}}(\mathbf{p}) P_s(\mathbf{k}-\mathbf{p}) \\ + \left[\frac{-i}{(2\pi)^d}\right]^2 P_s(\mathbf{k}) \int d\mathbf{p} d\mathbf{q} \mathbf{k}\cdot\hat{\mathbf{u}}(\mathbf{p}) P_s(\mathbf{k}-\mathbf{p}) \\ \times((\mathbf{k}-\mathbf{p})\cdot\hat{\mathbf{u}}(\mathbf{q})) P_s(\mathbf{k}-\mathbf{p}-\mathbf{q}),\end{aligned} \tag{A4}$$

where $P_s(\mathbf{k})$ and $\hat{\mathbf{u}}(\mathbf{p})$ are defined in [18]. Averaging over disorder and noting that

$$\langle \hat{\mathbf{u}} \rangle = 0,$$

$$\langle \hat{u}_i(\mathbf{p}) \hat{u}_j(\mathbf{q}) \rangle = p_i p_j \delta(\mathbf{p}+\mathbf{q}) (2\pi)^d \hat{E}(\mathbf{p}), \tag{A5}$$

we obtain

$$\begin{aligned}\langle \bar{c}(\mathbf{k},s) \rangle = P_s(\mathbf{k}) - \frac{1}{(2\pi)^d} \int d\mathbf{p} P_s^2(\mathbf{k}) (\mathbf{k}\cdot\mathbf{p})[\mathbf{p}\cdot(\mathbf{k}-\mathbf{p})] \\ \times \hat{E}(\mathbf{p}) P_s(\mathbf{k}-\mathbf{p}).\end{aligned} \tag{A6}$$

The thermal average of the particle position can be determined from this concentration via the relation

$$\overline{\langle \mathbf{x} \rangle} = \mathcal{L}\{\langle \mathbf{x} \rangle(t)\} = i \left.\frac{\partial \bar{c}}{\partial \mathbf{k}}\right|_{\mathbf{k}=0}, \tag{A7}$$

where the moment theorem of the Fourier transform has been used. Upon differentiating Eq. (A4), we get

$$\overline{\langle x_j \rangle} = \frac{1}{s^2}\left[F_j + \frac{i}{(2\pi)^d} \int d\mathbf{p} \frac{\hat{E}(\mathbf{p}) p_j p^2}{s + p^2\mathcal{T} - i\mathbf{p}\cdot\mathbf{F}}\right]. \tag{A8}$$

In order to find the long-time behavior, we expand the integrand for small $s$ and then perform the inverse Laplace transform, which leads to one of the required asymptotic forms

$$\begin{aligned}\langle x_j \rangle \sim t\left[F_j + \frac{i}{(2\pi)^d} \int d\mathbf{p} \hat{E}(\mathbf{p}) \frac{p^2 p_j}{p^2\mathcal{T} - i\mathbf{p}\cdot\mathbf{F}}\right] \\ - \frac{i}{(2\pi)^d} \int d\mathbf{p} \hat{E}(\mathbf{p}) \frac{p^2 p_j}{(p^2\mathcal{T} - i\mathbf{p}\cdot\mathbf{F})^2} + o(1) \\ = b_1^j t + b_0^j + o(1) \quad \text{as} \quad t \to \infty.\end{aligned} \tag{A9}$$

To find the coefficients $a_1$ and $a_2$, we calculate the second moment from the relation

$$\overline{\langle x_i x_j \rangle} = -\left.\frac{\partial^2 \bar{c}}{\partial k_i \partial k_j}\right|_{\mathbf{k}=0}, \tag{A10}$$

which after some calculation yields

$$\begin{aligned}\overline{\langle x_i x_j \rangle} = \frac{2\delta_{ij} T}{s^2} + \frac{2F_i F_j}{s^3} + \frac{2}{(2\pi)^d} \int d\mathbf{p} \hat{E}(\mathbf{p}) p_i \\ \times \frac{\partial}{\partial k_j}[P_s^2(\mathbf{k})(\mathbf{k}-\mathbf{p})\cdot\mathbf{p} P_s(\mathbf{k}-\mathbf{p})]|_{\mathbf{k}=0}.\end{aligned} \tag{A11}$$

The derivative in the integrand can be split into three terms,

$$\frac{\partial}{\partial k_j}[P_s^2(\mathbf{k})(\mathbf{k}-\mathbf{p})\cdot\mathbf{p} P_s(\mathbf{k}-\mathbf{p})]|_{\mathbf{k}=0} = T_1 + T_2 + T_3, \tag{A12}$$

with

$$\begin{aligned}T_1 &= -2P_s(\mathbf{0}) \frac{\partial P_s}{\partial k_j}(\mathbf{0}) p^2 P_s(-\mathbf{p}), \\ T_2 &= P_s^2(\mathbf{0}) p_j P_s(-\mathbf{p}), \\ T_3 &= -P_s^2(\mathbf{0}) p^2 \frac{\partial P_s}{\partial k_j}(-\mathbf{p}),\end{aligned} \tag{A13}$$

which we consider separately.

The first term can be written as

$$T_1 = 2\frac{1}{s}\left(\frac{-iF_j}{s^2}\right)(-p^2)\frac{1}{s + p^2\mathcal{T} - i\mathbf{p}\cdot\mathbf{F}} \tag{A14}$$

and gives a contribution to Eq. (A1) as $t \to \infty$ of

$$\begin{aligned}t^2\left[\frac{2i}{(2\pi)^d} \int d\mathbf{p} \hat{E}(\mathbf{p}) p_i \frac{p^2 F_j}{p^2\mathcal{T} - i\mathbf{p}\cdot\mathbf{F}}\right] \\ + t\left[-\frac{2i}{(2\pi)^d} \int d\mathbf{p} \hat{E}(\mathbf{p}) p_i \frac{2p^2 F_j}{(p^2\mathcal{T} - i\mathbf{p}\cdot\mathbf{F})^2}\right] + o(t).\end{aligned}$$

The second term is

$$T_2 = \frac{p_j}{s^2}\left(\frac{1}{s + p^2\mathcal{T} - i\mathbf{p}\cdot\mathbf{F}}\right) \tag{A15}$$

and gives a contribution to Eq. (A1) as $t \to \infty$ of

$$t\left[\frac{2}{(2\pi)^d} \int d\mathbf{p} \hat{E}(\mathbf{p}) \frac{p_i p_j}{p^2\mathcal{T} - i\mathbf{p}\mathbf{F}}\right] + o(t).$$

The final term is

$$T_3 = \frac{p^2}{s^2}\frac{(-2p_j\mathcal{T}+iF_j)}{(s+p^2\mathcal{T}-i\mathbf{p}\cdot\mathbf{F})^2}, \tag{A16}$$

whose contribution to Eq. (A1) as $t\to\infty$ is

$$t\left[\frac{2}{(2\pi)^d}\int d\mathbf{p}\hat{E}(\mathbf{p})p^2p_i\frac{-2p_j\mathcal{T}+iF_j}{(p^2\mathcal{T}-i\mathbf{p}\mathbf{F})^2}\right]+o(t).$$

Combining all the terms and performing the inverse Laplace transform, we obtain the required asymptotic form

$$\begin{aligned}\langle x_ix_j\rangle = t^2\left[F_iF_j+\frac{2i}{(2\pi)^d}\int d\mathbf{p}\frac{\hat{E}(\mathbf{p})p_ip^2F_j}{p^2\mathcal{T}-i\mathbf{p}\cdot\mathbf{F}}\right]\\ +t\left[2\delta_{ij}\mathcal{T}-\frac{2i}{(2\pi)^d}\int d\mathbf{p}\frac{2\hat{E}(\mathbf{p})p_ip^2F_j}{(p^2\mathcal{T}-i\mathbf{p}\cdot\mathbf{F})^2}\right.\\ +\frac{2}{(2\pi)^d}\int d\mathbf{p}\frac{\hat{E}(\mathbf{p})p_ip_j}{p^2\mathcal{T}-i\mathbf{p}\cdot\mathbf{F}}\\ \left.+\frac{2}{(2\pi)^d}\int d\mathbf{p}\hat{E}(\mathbf{p})p^2p_i\frac{(-2p_j\mathcal{T}+iF_j)}{(p^2\mathcal{T}-i\mathbf{p}\cdot\mathbf{F})^2}\right]+o(t)\\ = t^2a_2^{ij}+ta_1^{ij}+o(t).\end{aligned} \tag{A17}$$

Neglecting terms of order $(\hat{E})^2$ (since they correspond to the next order in the perturbation expansion), we get from Eqs. (A9) and (A17)

$$a_2^{ij}-b_1^ib_1^j=0, \tag{A18}$$

as we wanted to prove. On the other hand, the linear term in Eq. (A17) combined with Eq. (A9) yields

$$\begin{aligned}a_1^{ij}-b_0^ib_1^j-b_0^jb_1^i = 2\delta_{ij}\mathcal{T}+\frac{2}{(2\pi)^d}\int d\mathbf{p}\hat{E}(\mathbf{p})\\ \times\frac{p_ip_j(p^2\mathcal{T}-i\mathbf{p}\cdot\mathbf{F})-2p_ip_j\mathcal{T}p^2}{(p^2\mathcal{T}-i\mathbf{p}\cdot\mathbf{F})^2}.\end{aligned} \tag{A19}$$

Setting $D_{ij}$ to be half of this as per Eq. (A3), we arrive at the final expression

$$D_{ij}=\mathcal{T}\left[\delta_{ij}+\frac{\mathcal{T}}{(2\pi)^d}\int d\mathbf{p}\hat{E}(\mathbf{p})p^2\frac{p_ip_j[3(\mathbf{p}\cdot\mathbf{F})^2-\mathcal{T}^2p^4]}{[p^4\mathcal{T}^2+(\mathbf{p}\cdot\mathbf{F})^2]^2}\right]. \tag{A20}$$


[1] T. A. J. Duke and R. H. Austin, Phys. Rev. Lett. **80**, 1552 (1998).
[2] C. Reichhardt and F. Nori, Phys. Rev. Lett. **82**, 414 (1999); C. Reichhardt and C. J. Olson Reichhardt, Phys. Rev. E **69**, 041405 (2004); Europhys. Lett. **68**, 303 (2004).
[3] P. T. Korda, M. B. Taylor, and D. G. Grier, Phys. Rev. Lett. **89**, 128301 (2002).
[4] D. Grier, Nature (London) **424**, 810 (2003).
[5] A. Gopinathan and D. G. Grier, Phys. Rev. Lett. **92**, 130602 (2004).
[6] M. P. MacDonald, G. C. Spalding, and K. Dholakla, Nature (London) **426**, 421 (2003).
[7] L. R. Huang, E. C. Cox, R. H. Austin, and J. C. Sturm, Anal. Chem. **75**, 6963 (2003); Science **304**, 987 (2004).
[8] K. Ladavac, K. Kasza, and D. G. Grier, Phys. Rev. E **70**, 010901(R) (2004).
[9] M. Pelton, K. Ladavac, and D. G. Grier, Phys. Rev. E **70**, 031108 (2004).
[10] M. Khoury, A. M. Lacasta, J. M. Sancho, A. H. Romero, and K. Lindenberg, Phys. Rev. B **78**, 155433 (2008).
[11] K. Morton *et al.*, Proc. Natl. Acad. Sci. U.S.A. **105**, 7434 (2008).
[12] D. Speer, R. Eichhorn, and P. Reimann, Phys. Rev. Lett. **102**, 124101 (2009).
[13] A. M. Lacasta, J. M. Sancho, A. H. Romero, and K. Lindenberg, Phys. Rev. Lett. **94**, 160601 (2005).
[14] K. Lindenberg, A. M. Lacasta, J. M. Sancho, and A. H. Romero, New J. Phys. **7**, 29 (2005).
[15] K. Lindenberg, A. M. Lacasta, J. M. Sancho, and A. H. Romero, Proc. SPIE **5845**, 201 (2005).
[16] J. M. Sancho, M. Khoury, K. Lindenberg, and A. M. Lacasta, J. Phys.: Condens. Matter **17**, S4151 (2005).
[17] A. M. Lacasta, M. Khoury, J. M. Sancho, and K. Lindenberg, Mod. Phys. Lett. B **20**, 1427 (2006).
[18] J. P. Gleeson, J. M. Sancho, A. M. Lacasta, and K. Lindenberg, Phys. Rev. E **73**, 041102 (2006).
[19] J. P. Gleeson and D. I. Pullin, Phys. Fluids **15**, 3546 (2003).
[20] P. Reimann, C. Van den Broeck, H. Linke, P. Hänggi, J. M. Rubi, and A. Pérez-Madrid, Phys. Rev. E **65**, 031104 (2002).
[21] G. Costantini and F. Marchesoni, Europhys. Lett. **48**, 491 (1999).